Phonon enhancement of electronic order and negative isotope effect in the Hubbard-Holstein model on a square lattice

Da Wang,[1,*] Wan-Sheng Wang,[1] and Qiang-Hua Wang[1,2,†]

[1]*National Laboratory of Solid State Microstructures & School of Physics, Nanjing University, Nanjing, 210093, China*

[2]*Collaborative Innovation Center of Advanced Microstructures, Nanjing University, Nanjing 210093, China*

(Received 8 March 2015; revised manuscript received 14 October 2015; published 2 November 2015)

In phonon mediated conventional s-wave superconductors, higher-frequency phonon (or smaller atomic mass) leads to a higher superconducting transition temperature, known as the isotope effect. However, in correlated systems, various competing electronic order (such as spin-density-wave, charge-density-wave, and unconventional superconductivity) arises and the effect of electron-phonon coupling on these orders is a long-standing problem. Using the functional renormalization group, here we investigated the interplay between the electron correlation and electron-phonon coupling in the Hubbard-Holstein model on a square lattice. At half-filling, we found spin-density-wave and charge-density-wave phases and the transition between them, while no superconducting phase arises. Upon finite doping, d-wave/s-wave superconductivity emerges in proximity to the spin-density-wave/charge-density-wave phase. Surprisingly, lower-frequency Holstein phonons are either less destructive or even beneficial to the various phases, resulting in a negative isotope effect. For the superconducting phases, such an effect is apparently beyond the Bardeen-Cooper-Schrieffer theory.

DOI: 10.1103/PhysRevB.92.195102 PACS number(s): 71.38.−k, 74.20.Pq

I. INTRODUCTION

According to the standard Bardeen-Cooper-Schrieffer (BCS) theory of superconductivity [1], the only possible instability of a metallic normal state, described by the Landau-Fermi liquid, is the Cooper pairing toward superconductivity (SC) upon an attractive interaction [2]. The electron-phonon coupling (EPC) can mediate a retarded attractive interaction between electrons. This has to withstand the repulsive Coulomb interaction. Fortunately in conventional metals, the long-range Coulomb interaction is well screened and can be effectively replaced by a pseudopotential for quasiparticles below the energy scale of the Debye frequency ω_D [3,4]. The transition temperature T_c increases (linearly at weak coupling) with ω_D, known as the isotope effect. This has been a guiding principle in the search of superconductors with higher T_c, provided that EPC is the pairing glue. However, the simple BCS scenario could break down in many ways. When the Fermi surface touches van Hove singularities, or is nested, density waves in the spin or charge channel would be favorable. A well-known example is the Peierls instability toward the charge-density-wave (CDW) phase in one-dimensional (1D) electron systems with EPC alone [5]. In correlated electrons systems, the local interactions are poorly screened, leaving the various orders, such as the spin-density-wave (SDW), CDW, and unconventional SC, close competitors to each other, when the Fermi surface is featured with van Hove singularities and/or nesting. In the Mott limit, the strong local interaction leads to the formation of local spin moments in the first place. The effect of EPC in such cases is an intriguing issue. For example, a long-standing question is whether EPC plays a significant role for d-wave pairing in copper-based [6–8] and $s_{\pm}$-wave pairing in iron-based high-temperature superconductors [9]. As a first step toward the issue, one considers theoretically a simplest model with local Holstein phonons and local Hubbard interactions, the so-called Hubbard-Holstein model (HHM). Much effort has been devoted to understand the various orders and the metal-insulator transition in the HHM in 1D [10] and infinite dimensions [11,12]. In view of unconventional SC other than s-wave SC (s-SC), such as d-wave SC (d-SC) in layered materials, here we consider a HHM on a two-dimensional (2D) square lattice. We handle the interplay between electron correlation and EPC by the singular-mode functional renormalization group (SM-FRG) [13,14]. We limit ourselves to weak and moderate correlations [15,16] for which FRG has proved to be successful (see Refs. [17,18] and references therein). Our main findings are as follows. At half-filling, SDW and CDW compete, but no SC phase arises. Upon finite doping, d-SC/s-SC emerges in proximity to SDW/CDW phases. More interestingly, lower-frequency Holstein phonons are either less destructive, or even beneficial, to the various phases. Specifically, lower-frequency Holstein phonon enhances SDW/d-SC and s-SC in proximity to CDW, with an unusual negative isotope effect.

II. MODEL AND METHOD

The 2D HHM is described by the Hamiltonian,

$$H = -t\sum_{\langle ij\rangle\sigma}(c^{\dagger}_{i\sigma}c_{j\sigma} + \text{H.c.}) - \mu\sum_{i\sigma} n_{i\sigma} + \omega_D\sum_i b^{\dagger}_i b_i + U\sum_i\left(n_{i\uparrow}-\frac{1}{2}\right)\left(n_{i\downarrow}-\frac{1}{2}\right) + \eta\sum_{i\sigma} n_{i\sigma}(b^{\dagger}_i + b_i), \quad (1)$$

where t is the nearest-neighbor hopping, μ the chemical potential, U the local Hubbard interaction, ω_D the Holstein phonon frequency, and $\eta = g/\sqrt{2M\omega_D}$. Here g is the EPC matrix element and M is the mass of the vibrating ion. Henceforth we set $t = 1$ as the unit of energy. The EPC leads to a retarded attraction $\Pi_\nu = -\lambda W\omega_D^2/(\omega_D^2 + \nu^2)$, where ν is the

*dawang@nju.edu.cn
†qhwang@nju.edu.cn

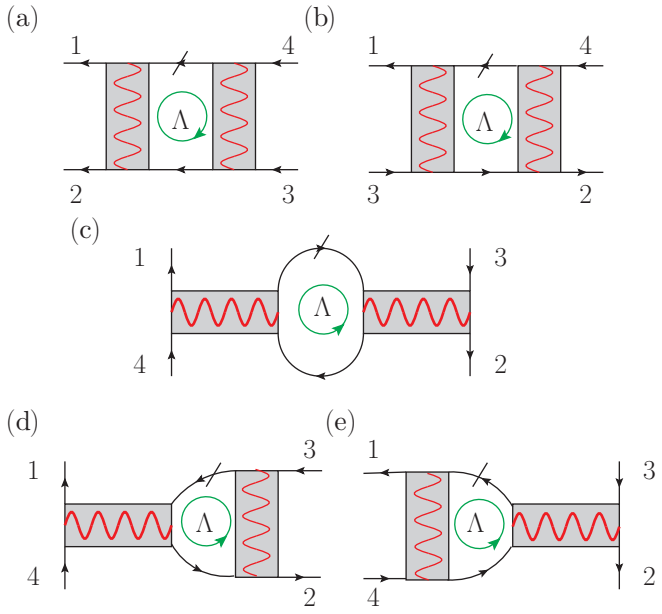

FIG. 1. (Color online) One-loop contributions to $d\Gamma_\Lambda^{1234}/d\Lambda$. The grayed bar and thin (thick) wavy line denote Γ_Λ and Π_Λ (Π_0), respectively. Spin is conserved during fermion propagation and is left implicit. The slash denotes the single-scale propagator and can be put on either one of the fermion lines within the loop. The directed-circle indicates circulation of frequency at the scale of Λ.

Matsubara frequency, $W = 8$ the electron bandwidth, and $\lambda = g^2/(M\omega_D^2 W)$ an average EPC constant which depends on the spring constant $K = M\omega_D^2$ rather than on ω_D independently. We notice that $\Pi_0 = -\lambda W$ is the characteristic energy scale of the phonon-mediated attraction.

We treat the correlation effect and EPC by the SM-FRG [13,14]. Here we outline the necessary ingredients and notations, leaving technical details in Appendix A. In a nutshell, the idea is to get momentum-resolved pseudopotential $\Gamma_{\Lambda,1234}$, as in $(1/2)c_{1\sigma}^\dagger c_{2\sigma'}^\dagger \Gamma_{\Lambda,1234} c_{3\sigma'} c_{4\sigma}$, to act on low-energy fermionic degrees of freedom up to a cutoff energy scale Λ (for Matsubara frequency in our case). Henceforth the numerical index labels momentum/position (but will be suppressed wherever applicable for brevity). Momentum conservation/translation symmetry is also left implicit. The FRG flow $d\Gamma_\Lambda/d\Lambda$ is contributed by the Feynman diagrams shown in Fig. 1. The initial condition $\Gamma_{\Lambda\to\infty}$ is specified by the bare interaction U. Since $d\Gamma_\Lambda/d\Lambda$ depends on Γ_Λ itself and $\Pi_{\nu=0,\Lambda}$, as seen in Fig. 1, the integration towards lower Λ generates all one-particle-irreducible corrections to arbitrary orders in terms of the bare interactions U and Π_ν. As Λ is lowered, Γ_Λ can evolve to be nonlocal and even diverging. To see the instability (diverging) channel, we extract concurrently the effective interactions in the general CDW/SDW/SC channels,

$$\begin{aligned}
\left[V_\Lambda^{\rm CDW}\right]_{(14)(32)} &= 2[\Gamma_\Lambda + \Pi_0]_{1234} - [\Gamma_\Lambda + \Pi_\Lambda]_{1243},\\
\left[V_\Lambda^{\rm SDW}\right]_{(13)(42)} &= -[\Gamma_\Lambda + \Pi_\Lambda]_{1234},\\
\left[V_\Lambda^{\rm SC}\right]_{(12)(43)} &= [\Gamma_\Lambda + \Pi_\Lambda]_{1234}.
\end{aligned} \tag{2}$$

Notice that $\Pi_{\nu=0,\Lambda}$ is local/flat in real/momentum space for Holstein phonons. The left-hand sides are understood as matrices with composite indices, describing scattering of fermon bilinears. Since they all originate from Γ_Λ and Π_ν, $V_\Lambda^{\rm CDW/SDW/SC}$ have overlaps but are naturally treated on equal footing. The divergence of the leading attractive (i.e., negative) eigenvalue of $V_\Lambda^{\rm CDW/SDW/SC}$ decides the instability channel, the associated eigenfunction and collective momentum describe the order parameter, and the divergence energy scale Λ_c is representative of the transition temperature T_c.

III. RESULTS

Before embarking on full-wedge FRG results, we digress to gain qualitative insights first from a local approximation: We keep the local part of Γ_Λ only so that the FRG reduces to a simple RG. We focus on half-filling, where the particle-hole symmetry enables us to solve Γ_Λ analytically (see Appendix A 3),

$$\Gamma_\Lambda + \Pi_0 \sim (U + \Pi_0) \exp\left[\frac{\alpha\lambda W}{\omega_D}\left(1 - \frac{2}{\pi}\tan^{-1}\frac{\Lambda}{\omega_D}\right)\right], \tag{3}$$

where α is a constant of order unity. The effective interactions in the local approximation are $(V_\Lambda^{\rm SC}, V_\Lambda^{\rm SDW}, V_\Lambda^{\rm CDW}) = (\Gamma_\Lambda + \Pi_\Lambda, -\Gamma_\Lambda - \Pi_\Lambda, \Gamma_\Lambda + 2\Pi_0 - \Pi_\Lambda)$. They are bounded, but their behaviors still provide interesting implications: (1) We observe that $V_\Lambda^{\rm SC} > V_\Lambda^{\rm CDW}$ for any $\lambda > 0$, so SC is absent at half-filling. In fact, even if $\lambda = 0$ the SC and CDW channels are exactly degenerate, satisfying the SO(4) = SU(2) $\otimes$ SU(2) symmetry [19] where the excess pseudo-SU(2) arises from the particle-hole symmetry at half-filling. (2) If $U + \Pi_0 = U - \lambda W = 0$, there is a fixed line $\Gamma_\Lambda = U$, on which $V_\Lambda^{\rm SDW} = V_\Lambda^{\rm CDW} < 0$. This implies a phase boundary between CDW and SDW. (The local interactions are dispersionless, but the nesting vector (π,π) decides the CDW/SDW wave vector.) (3) If $U - \lambda W > 0$ (or <0), Γ_Λ is driven more (or less) repulsive so that SDW (or CDW) can be enhanced by EPC. (4) A lower ω_D leads to stronger enhancement of $|\Gamma_\Lambda + \Pi_0|$, implying that softer phonons are beneficial for CDW and SDW in the respective phase regimes, resulting in a negative isotope effect for both orders. This effect can also be understood qualitatively from the quasiparticle point of view. Under the Lang-Firsov transform [20], $H \to \mathcal{U}H\mathcal{U}^\dagger$ where $\mathcal{U} = \exp[(\eta/\omega_D)\sum_i n_i(b_i - b_i^\dagger)]$, the electron operator $c_i \to c_i e^{-(\eta/\omega_D)(b_i - b_i^\dagger)}$, which is a polaron operator. By averaging over the phonon ensemble, one obtains a coherent bandwidth narrowed by a factor of

$$z = \exp\left[-\frac{\lambda W}{2\omega_D}\frac{1 + e^{\beta\omega_D}}{e^{\beta\omega_D} - 1}\right], \tag{4}$$

where $\beta{=}1/T$ is the inverse temperature. To sustain the quasiparticle coherence one requires $T \ll \omega_D$ so that phonon excitations are rare. On the other hand, $U \to U - \lambda W$ after the Lang-Firsov transform. The interaction to bandwidth ratio becomes $r = (U/W - \lambda)/z$. This ratio is amplified by $1/z$ as long as $|U - \lambda W| \neq 0$, implying a phase boundary $U - \lambda W = 0$ between CDW and SDW. More interestingly, the amplifying factor $1/z$ is in nice agreement with the exponential factor in Eq. (3) in the limit of $\Lambda \ll \omega_D$, a condition consistent with $T \ll \omega_D$ mentioned above. The negative isotope effect uncovered above are therefore exactly a manifestation of the

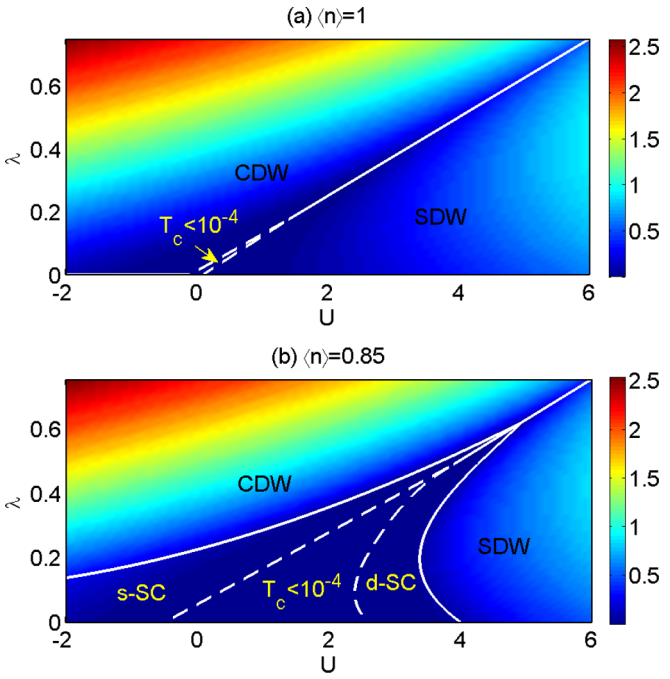

FIG. 2. (Color online) Phase diagrams for (a) $\langle n\rangle = 1$ and (b) $\langle n\rangle = 0.85$. The color encodes the transition temperature T_c. The dashed lines enclose the regime in which $T_c < 10^{-4}$. Here $\omega_D = 0.5$.

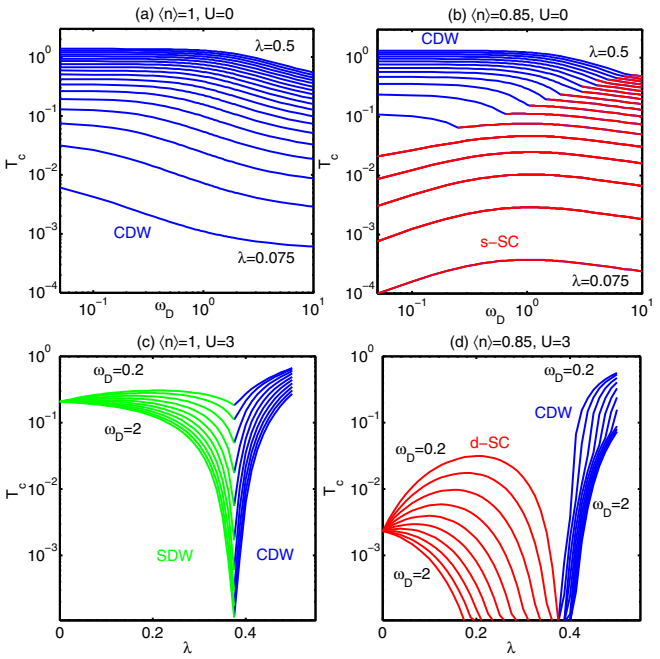

FIG. 3. (Color online) T_c versus λ and ω_D with $U = 0$ in (a) and (b), and $U = 3$ in (c) and (d). The phases are denoted by both text and color. The solid lines are equally spaced by $\Delta\lambda = 0.025$ in (a) and (b), and $\Delta\omega_D = 0.2$ in (c) and (d).

fact that the polaronic effect is stronger for softer phonons. We should caution that the Lang-Firsov approximation applies best in the antiadiabatic limit $\omega_D \gg W$, but our RG result holds for general ω_D.

We now turn to the full-wedge FRG results by retaining the nonlocal part of Γ_Λ, and the emerging order is determined by the leading divergence in the various channels. Figure 2 is the phase diagram for $\omega_D = 0.5$ for two filling levels. The color encodes T_c versus U and λ. The dashed lines enclose a regime in which $T_c < 10^{-4}$ beyond our interest. At half-filling $\langle n\rangle = 1$ in Fig. 2(a), there is a phase boundary $U = \lambda W$ separating the CDW and SDW phases. In the CDW phase, T_c is enhanced with increasing λ. In the SDW regime, T_c exhibits a dome-shaped behavior along the λ axis, implying that a weak λ also enhances SDW. These behaviors are exactly what we discussed and understood in the above simple RG analysis. Moreover, the full FRG is able to capture general pairing channels. For example, in the SDW phase, $V_{\rm SC}$ has a negative eigenvalue in the d-wave pairing channel, but it is always less diverging than that of $V_{\rm SDW}$. This excludes d-SC at half-filling. The phase diagram is in good agreement with the quantum Monte Carlo (QMC) result [21] on finite-size lattices, demonstrating the reliability of our FRG.

Away from half-filling, our result for $\langle n\rangle = 0.85$ is shown in Fig. 2(b). Since the perfect nesting is no longer at the Fermi level, the CDW (SDW) order with wave vector is stabilized beyond a finite threshold $\lambda > \lambda_c$ ($U > U_c$). Their wave vector is still found to be (π,π) because the SDW/CDW interactions are established by virtual particle-hole excitations at energy scales higher than the small shift of Fermi level. Below the phase boundary of CDW, we find s-SC is established. On the other hand, near the SDW phase boundary, d-SC emerges. The proximity between these phases is easily understood in view of the overlap between the SDW and SC channels, and is also known as a manifestation of pairing induced by SDW fluctuations [22,23]. What's more interesting here is the phase boundaries of both SDW and d-SC phases are curvy in the parameter space, implying that weak (strong) EPC enhances (suppresses) both SDW and d-SC. Given the behavior of SDW versus EPC we discussed above, however, the anomalous enhancement becomes natural in view of the overlap between SDW and d-SC channels. We notice that in an earlier FRG work [24], the EPC (with Holstein phonons) appears to suppress d-SC. We ascribe the difference to the dilute frequencies (with minimal frequency spacing much larger than Debye frequency) used for Π_ν in their case.

We now check more systematics for the effects of EPC on T_c of the various phases. For a pure EPC system with $U = 0$, the transition temperature T_c is shown in Figs. 3(a) and 3(b). At half-filling in (a), only CDW phase is present, and T_c clearly drops with increasing ω_D, for any λ. Such a negative isotope effect is discussed above, and is in agreement with the result judged from correlation functions measured by QMC on small clusters [25]. For $\langle n\rangle = 0.85$ in (b), the CDW phase is realized for large λ, and T_c follows the trend in (a) closely. For weaker λ, the system yields to the s-SC phase. In proximity to the CDW phase, we observe that T_c for s-SC drops for larger ω_D. This is understood as caused by the weakening of CDW fluctuations, so that T_c for s-SC eventually inherits a negative isotope effect. For even weaker λ, however, T_c for s-SC increases with small ω_D, in a BCS fashion. In fact, the FRG reproduces the exact BCS behavior $T_c \propto \omega_D$ for $\lambda \to 0$ and $\omega_D \ll W$, if the CDW and SDW channels are too weak to

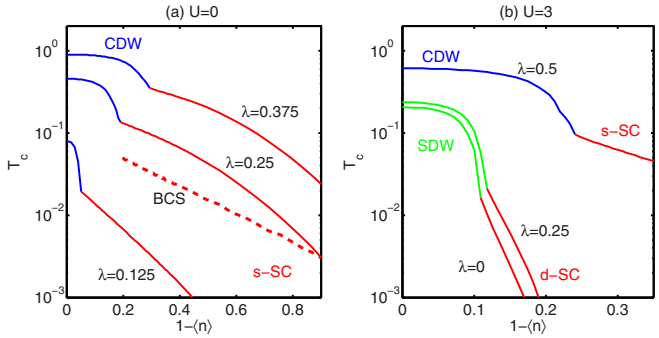

FIG. 4. (Color online) Doping dependence of T_c for $\omega_D = 0.5$ and $U = 0$ (a) and $U = 3$ (b). The phases are denoted by both text and color. The dashed line in (a) is a fit to the BCS theory (see the text for more details).

affect the pairing channel. We have numerically checked this point, and an analytic derivation can be found in Appendix A 2. Therefore, the negative isotope effect for s-SC occurs only in proximity to the CDW phase.

For a correlated system with $U = 3$, the transition temperature T_c is shown in Figs. 3(c) and 3(d). At half-filling in (c), a large λ drives SDW into CDW, with a phase transition at $\lambda_c = U/W$ independent of ω_D. The transition temperature is always lower for larger ω_D, again a manifestation of the negative isotope effect. Moreover, we observe in (c) a slight enhancement of SDW by a weak λ at small ω_D. This effect is qualitatively explained by Eq. (3), and has been discussed previously. To our delight, the slight enhancement is consistent with the DCA result for $U = W = 8$ in Ref. [26]. For the doped case, as $\langle n\rangle = 0.85$ in Fig. 3(d), the SDW phase yields to the d-SC phase, and the CDW phase remains for large λ. Here T_c is laterally higher for lower ω_D for both CDW and d-SC in the respective regimes. A similar case was observed but only for the d-SC phase in Ref. [27]. Moreover, in the d-SC regime, even though T_c decreases with λ for $\omega_D > 1$, it is lifted by a lower ω_D for a given λ. Thus lower-frequency phonons are at least less destructive to the d-SC. On the other hand, there is a marked enhancement of T_c by a weak λ, up to $\lambda = 0.2$ for $\omega_D = 0.2$, which we ascribe to the anomalous enhancement of SDW fluctuations as revealed in Fig. 3(c). The reason that the negative isotope effect is observed in the entire d-SC regime is because d-SC occurs only in proximity to the SDW phase.

Finally, we consider the systematics in doping. We set $\omega_D = 0.5$ for illustration. For $U = 0$, Fig. 4(a) shows the CDW phase is present at low doping, and s-SC at higher doping. For stronger λ, a larger doping is needed to enter the s-SC phase. In both phases, T_c decreases with doping, since the density of states ρ at the Fermi level drops. We compare our result to the BCS formula (dashed line), $T_c^{\rm BCS} = 1.13\omega_D \exp(-1/\rho V_{\rm BCS})$ [1]. We choose the value of $V_{\rm BCS}$ so that $T_c^{\rm BCS}$ matches our FRG result for $\lambda = 0.25$ and a deep doping level $1 - \langle n\rangle = 0.9$. We find $T_c > T_c^{\rm BCS}$ approaching half-filling. The enhancement follows from the effect of increasing CDW fluctuations, also favorable for s-wave pairing but missing in the simple BCS theory. For a nonzero $U = 3$ in Fig. 4(b), the CDW and s-SC phases are realized if λ is sufficiently large (e.g., $\lambda = 0.5$). For a weaker $\lambda = 0.25$, d-SC sets in since the SDW fluctuations become stronger. Closer to half-filling, the SDW phase eventually sets in. For both phases, T_c is higher for $\lambda = 0.25$ than that for $\lambda = 0$, reconfirming the previous result that a weak EPC enhances SDW/d-SC if ω_D is small.

IV. SUMMARY AND DISCUSSION

In summary, we investigated the effects of EPC in a 2D HHM systematically by SM-FRG. We found lower-frequency Holstein phonons are beneficial to all of CDW, SDW, and s-SC/d-SC in proximity to CDW/SDW phases, resulting in a negative isotope effect. The qualitative mechanism is as follows. For CDW, low-frequency phonons can be easily softened and adapt to the CDW order. Near the phase boundary of CDW, the enhanced CDW fluctuations are beneficial to s-SC. For SDW and d-SC, the enhancement can be effectively ascribed to polaronic band narrowing, which in turn blows up the correlation effect, favoring SDW and the d-SC in its proximity.

Before closing, a few remarks are in order. First, in a strict 2D system, academically there is no finite temperature SDW phase by the Mermin-Wagnar theorem [28], and there is only algebraic SC order below the Kosterlitz-Thouless temperature [29]. In this regard, T_c in our case should be understood as a crossover temperature in 2D, or the transition temperature in quasi-2D systems. Second, we stress again that FRG is perturbative in nature, and it works best in the itinerant picture up to moderate $U/W \sim 1$ and $\lambda \sim 1$, as discussed in this paper. While in the strong correlation limit, EPC might also enhance the T_c of SDW [26] as a result of self-localization of polarons in the presence of a sufficiently strong EPC [26,30–35]. On the other hand, we notice that whether EPC would enhance d-SC in the strong correlation limit is under debate [36,37]. Furthermore, the negative isotope effect of the d-SC observed here (also confirmed by an early study [27]) may become positive in the strong correlation limit [38]. Finally, there is even a proposal that EPC-driven bipolarons are necessary ingredients for high-T_c SC in cuprates [8].

ACKNOWLEDGMENTS

The project was supported by NSFC (under Grants No. 11574134 and No. 11504164) and the Ministry of Science and Technology of China (under Grants No. 2011CBA00108 and No. 2011CB922101). W.S.W. also thanks the support of the China Postdoctoral Science Foundation (under Grant No. 2014M561616). The numerical calculations were performed at the High Performance Computing Center of Nanjing University.

APPENDIX A: TECHNICAL DETAILS OF SM-FRG

Consider the interaction Hamiltonian $H_I = (1/2)c^\dagger_{1\sigma}c^\dagger_{2\sigma'}\Gamma_{1234}c_{3\sigma'}c_{4\sigma}$. Here the numerical index labels momentum/position, and we leave implicit the momentum conservation/translation symmetry. The spin SU(2) symmetry is guaranteed in the above convention for H_I. The idea of FRG is to get the one-particle-irreducible interaction vertex Γ for fermions whose energy/frequency is above a scale Λ. (Thus Γ is Λ dependent.) Equivalently, such an effective

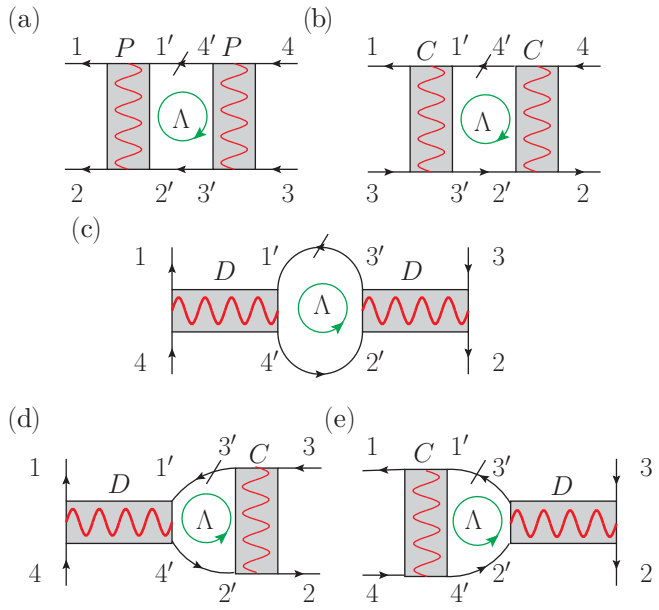

FIG. 5. (Color online) One-loop contributions to $\partial\Gamma_{1234}/\partial\Lambda$. The grayed bar and thin (thick) wavy line denote Γ_Λ and Π_Λ (Π_0), respectively. They are added up wherever overlayed. Spin is conserved during fermion propagation and is left implicit. The slash denotes the single-scale propagator and can be put on either one of the fermion lines within the loop. The directed-circle indicates circulation of frequency along the loop, and Λ the running scale. Each diagram can be viewed as a convolution of aliases of Γ (together with Π_v) via $\Gamma_{1234} = P_{(12)(43)} = C_{(13)(42)} = D_{(14)(32)}$.

interaction is what's called pseudopotential for fermions whose energy/frequency is below Λ. Starting from the local U at $\Lambda = \infty$, the contributions to $\partial\Gamma/\partial\Lambda$ are illustrated in Fig. 5. In principle there will also be self-energy correction to fermions, which we ignore as usual, given the fact that we are just looking for the instability of the normal state. To proceed, it is useful to define matrix aliases of the rank-4 "tensor" Γ via

$$\Gamma_{1234} = P_{(12)(43)} = C_{(13)(42)} = D_{(14)(32)}. \tag{A1}$$

Then $\partial\Gamma/\partial\Lambda$ can be compactly written as

$$\begin{aligned}\frac{\partial\Gamma_{1234}}{\partial\Lambda} = {} & [\mathcal{D}\chi^{ph}(\mathcal{D}-\mathcal{C}) + (\mathcal{D}-\mathcal{C})\chi^{ph}\mathcal{D}]_{(14)(32)} \\ & + [\mathcal{P}\chi^{pp}\mathcal{P}]_{(12)(43)} - [\mathcal{C}\chi^{ph}\mathcal{C}]_{(13)(42)},\end{aligned} \tag{A2}$$

where matrix convolutions are understood within the square brackets, and

$$\begin{aligned}\mathcal{P} = P + \Pi_\Lambda,\ \mathcal{C} = C + \Pi_\Lambda,\ \mathcal{D} = D + \Pi_0, \\ \chi^{pp}_{(ab)(cd)} = \frac{1}{2\pi}[G_{ac}(\Lambda)G_{bd}(-\Lambda) + (\Lambda \to -\Lambda)], \\ \chi^{ph}_{(ab)(cd)} = -\frac{1}{2\pi}[G_{ac}(\Lambda)G_{db}(\Lambda) + (\Lambda \to -\Lambda)],\end{aligned} \tag{A3}$$

where $\Pi_\Lambda = -\lambda W\omega_D^2/(\omega_D^2 + \Lambda^2)$ and $\Pi_0 = -\lambda W$ as defined in the main text. Both Π_Λ and Π_0 enter as a matrix (local in real space and flat in momentum space), G is the normal state Green's function, and we used a hard cutoff in the continuous Matsubara frequency [39]. Notice that Π_0 enters $\mathcal{D}$ because the EPC-induced interaction is direct in the charge channel. This is also evident from Fig. 5. Since the external lines are set at zero frequency (the frequency dependence is irrelevant for four-point interactions in the RG sense), the frequency on the phonon lines (thickened wavy lines) overlayed by D is automatically zero in Figs. 5(c)–5(e).

The integration of $\partial\Gamma/\partial\Lambda$ toward decreasing Λ generates all one-particle-irreducible corrections to Γ from U and Π_v to arbitrary orders. From Γ (or its aliases P, C, and D), Π_Λ and Π_0, we extract concurrently the effective interactions in the general SC/SDW/CDW channels,

$$(V^{\rm SC}, V^{\rm SDW}, V^{\rm CDW}) = (\mathcal{P}, -\mathcal{C}, 2\mathcal{D} - \mathcal{C}). \tag{A4}$$

They are matrices describing scattering of fermion bilinears in the respective channels, equivalent to Eq. (2) in the main text. Since they all originate from Γ, Π_Λ, and Π_0, they are overlapped but are naturally treated on equal footing. The effective interactions can be decomposed into eigenmodes. For example, in the SC channel (with a zero collective momentum),

$$[V^{\rm SC}]_{(\mathbf{k},-\mathbf{k})(\mathbf{k}',-\mathbf{k}')} = \sum_m f_m(\mathbf{k}) S_m f_m^*(\mathbf{k}'), \tag{A5}$$

where S_m is the eigenvalue, and $f_m(\mathbf{k})$ is the eigenfunction. We look for the most negative eigenvalue, say $S = \min[S_m]$, with an associated eigenfunction $f(\mathbf{k})$. If S diverges at a scale Λ_c, it signals the instability of the normal state toward an SC state, with a pairing function described by $f(\mathbf{k})$. Similar analysis can be performed in the CDW/SDW channels, with the only exception that in general the collective momentum $\mathbf{q}$ in such channels is nonzero. Since $\mathbf{q}$ is a good quantum number in the respective channels, one performs the mode decomposition at each $\mathbf{q}$. There are multiple modes at each $\mathbf{q}$, but we are interested in the globally leading mode among all $\mathbf{q}$. In this way one determines both the ordering vector $\mathbf{Q}$ and the structure of the order parameter by the leading eigenfunction. Finally, the instability channel is determined by comparing the leading eigenvalues in the CDW/SDW/SC channels.

In principle, the above procedure is able to capture the most general candidate order parameters. In practice, however, it is impossible to keep all elements of the "tensor" Γ for computation. Fortunately, the order parameters are always local or short-ranged. This is notwithstanding the possible long-range correlations between the order parameters. For example, the s-wave pairing in the BCS theory is local, since the gap function is a constant in momentum space. The order parameter in usual Landau theories is assumed to be local. The d-wave pairing is nonlocal but short-ranged. The usual CDW/SDW orders are ordering of site-local charges/spins. The valence-bond order is on-bond but short-ranged. In fact, if the order parameter is very nonlocal, it is not likely to be stable. The idea is, if it is not an instability at the tree level, it has to be induced by the overlapping channel. But if the induced order parameter is very nonlocal, it must be true that the donor channel has already developed long-range fluctuations and is ready to order first. These considerations suggest that most elements of the "tensor" Γ are irrelevant in the RG sense and can be truncated. Equation (A2) suggests how this can be done. For fermions, all four-point interactions are marginal in the RG sense, and the only way a marginal operator

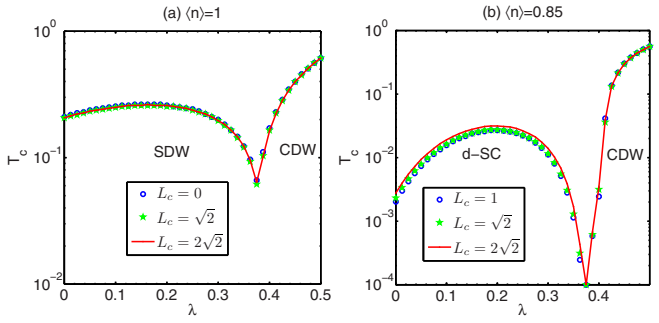

FIG. 6. (Color online) Dependence of our SM-FRG results on the truncation range L_c in both undoped and doped cases. In calculations, $U = 3$ is used.

could become relevant is through coherent and repeated scattering in a particular channel. Therefore, it is sufficient to truncate internal spatial range within the fermion bilinear, e.g., between 1 and 2, between 3 and 4, in $\mathcal{P}_{(12)(43)}$. The setback distance between the two groups is, however, unlimited (thus thermodynamical limit is not spoiled). Similar considerations apply to $\mathcal{C}$ and $\mathcal{D}$. Eventually the same type of truncations can be applied in the effective interactions $V^{\mathrm{CDW/SDW/SC}}$. Such truncations keep the potentially singular contributions in all channels and their overlaps, underlying the key idea of the SM-FRG [13,14,40]. The merit of SM-FRG is as follows: (1) It guarantees Hermiticity of the truncated interactions; (2) it is asymptotically exact if the truncation range is enlarged; (3) it respects all underlying symmetries, and in particular it respects momentum conservation exactly. (4) In systems with multiorbitals or complex unitcell, it is important to keep the momentum dependence of the Bloch states, both radial and tangential to the Fermi surface. This is guaranteed in SM-FRG since it works with Green's functions in the orbital basis. We take these as advantages of SM-FRG as compared to the patch FRG applied in the literature [17,18,39].

1. Convergence of the truncation range

To check the validity of the real-space truncation for fermion bilinears discussed above, we define L_c as the maximal distance between the two fermions within a fermion bilinear. We consider L_c from $L_c = 0$ (on site) up to $L_c = 2\sqrt{2}$ (fifth neighbor on the square lattice). The resulting diverging scale for various L_c's is shown in Fig. 6. At half-filling in (a), a longer $L_c > 0$ hardly affects the divergence scale Λ_c obtained for $L_c = 0$. This is because the order parameters of both SDW and CDW are site local in the present model. For the doped case $\langle n\rangle = 0.85$ in (b), the results for $L_c = \sqrt{2}$ and $L_c = 2\sqrt{2}$ are indistinguishable, signaling the convergence versus L_c. Notice that $L_c \geqslant 1$ is needed for d-SC since symmetry requires pairing on bond. In the main text, we used $L_c = \sqrt{2}$, which appears to be sufficient to take care of all orders in the present model.

2. BCS limit

We notice that if only Fig. 5(a), the pairing channel, is kept, the BCS theory is trivially reproduced. For this to be valid, one requires $\Lambda_c \ll \omega_D \ll W$ and the absence of any nesting, so that the contributions from the other channels, Figs. 5(b)–5(e), are negligible. To make analytical solution accessible, we approximate Π_ν as a step function, $\Pi_\nu = -\lambda W\theta(\omega_D - |\nu|)$. Thus $\Pi_\Lambda = 0$ for $\Lambda > \omega_D$, and the RG flow above ω_D merely generates a renormalized Coulomb interaction V^*. The flow for $\Lambda < \omega_D$ is, with $\Pi_\Lambda = -\lambda W$ in the above approximation,

$$\partial(V^{\mathrm{SC}} - \lambda W)/\partial\Lambda = (\rho/\Lambda)(V^{\mathrm{SC}} - \lambda W)^2, \qquad \text{(A6)}$$

where ρ is the normal state density of states, and we assumed that $V^{\mathrm{SC}}_{(\mathbf{k},-\mathbf{k})(\mathbf{k}',-\mathbf{k}')}$ is independent of $\mathbf{k}$ and $\mathbf{k}'$, as assumed in the BCS theory. (This means that we are treating on-site s-wave pairing.) The solution is, given the boundary condition at $\Lambda = \omega_D$,

$$V^{\mathrm{SC}} - \lambda W = \frac{V^* - \lambda W}{1 + (\lambda - \mu^*)\ln(\Lambda/\omega_D)}, \qquad \text{(A7)}$$

where we used $\mu^* = \rho V^*$ and $\rho W \sim 1$. There is a divergence $V^{\mathrm{SC}} - \lambda W \to -\infty$ if and only if $\lambda - \mu^* > 0$ (i.e., EPC mediated attraction overwhelms the repulsive V^*), at the scale,

$$\Lambda_c = \omega_D e^{-1/(\lambda-\mu^*)}. \qquad \text{(A8)}$$

This is already in nice agreement with the T_c in the Eliashberg theory, given the approximations in Π_ν. This example shows that the idea of pseudopotential can be pushed down to any energy scale (not just at ω_D as in the BCS theory) until it diverges, and the divergence scale is just a representative of the transition temperature T_c. If sufficiently strong, the CDW/SDW channels neglected in the BCS theory will clearly invalidate the latter, as revealed in the main text.

3. Local limit

On the other hand, if only the local elements of Γ are kept, we have $\Gamma = P = C = D$. Furthermore, in the presence of

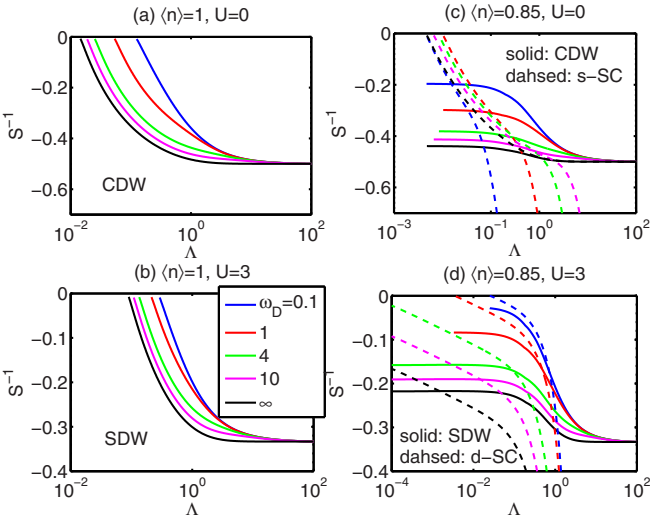

FIG. 7. (Color online) Effects of EPC on the flow of leading eigenvalues S (plotted as $1/S$ for clarity) of $V^{\mathrm{CDW/SDW/SC}}$ at $\lambda = 1/8$ for (a) $\langle n\rangle = 1$ and $U = 0$, (b) $\langle n\rangle = 1$ and $U = 3$, (c) $\langle n\rangle = 0.85$ and $U = 0$, and (d) $\langle n\rangle = 0.85$ and $U = 3$. The phonon frequency is indicated in the legend for all panels. For clarity, a channel is dropped if it's $|S|$ is too weak, and S is multiplied by a factor of 10 in the flow of SC channel in (d).

particle-hole symmetry (at half-filling in HHM), the second line of Eq. (A2) cancels out (in the local limit), leaving

$$\frac{\partial\Gamma}{\partial\Lambda} = -\frac{2}{\pi}(\Pi_0 - \Pi_\Lambda)\frac{\partial\chi_\Lambda}{\partial\Lambda}(\Gamma + \Pi_0), \tag{A9}$$

where $\chi_\Lambda \sim \alpha/\Lambda$ is a local susceptibility at the scale Λ, with a factor α of order unity. This can be solved analytically,

$$\Gamma + \Pi_0 \sim (U + \Pi_0)\exp\left[\frac{\alpha\lambda W}{\omega_D}\left(1 - \frac{2}{\pi}\tan^{-1}\frac{\Lambda}{\omega_D}\right)\right], \tag{A10}$$

where we used $\Pi_0 = -\lambda W$. This is Eq. (3) in the main text.

APPENDIX B: REPRESENTATIVE FRG FLOWS

In the main text, we present the divergence scale T_c in the various cases. Here we show how it is determined by presenting and discussing some representative FRG flows of the leading eigenvalues S of $V^{\mathrm{CDW/SDW/SC}}$ in Fig. 7 for $\lambda = 1/8$. Since we are looking for divergence, we drop out Π_0 and Π_Λ in Eq. (A4) to concentrate on the flow of the projections of Γ in the various channels. At half-filling with $U = 0/3$ in Figs. 7(a) and 7(b), the CDW and SDW channels, respectively, diverge as Λ is lowered. We have checked that for a pure negative-U Hubbard model, equivalent to $\omega_D = \infty$ and $U = 0$ in (a), the s-SC and CDW channels are exactly degenerate, satisfying the SO(4) = SU(2) ⊗ SU(2) symmetry [19], where the excess pseudo-SU(2) arises from the particle-hole symmetry at half-filling. However, a finite ω_D breaks the pseudo-SU(2) symmetry in favor of CDW [25], since Π_ν is a direct interaction in the charge channel. For both CDW and SDW channels, $1/S$ is higher for lower ω_D, and so is T_c. This is just the negative isotope effect.

For $\langle n\rangle = 0.85$ in Figs. 7(c) and 7(d), the CDW and SDW interaction flow, respectively, at high Λ is similar to that in Figs. 7(a) and 7(b) for half-filling, since high-energy quasiparticles are insensitive to the Fermi level. As Λ decreases further, however, low-energy quasiparticles come into play, but the lack of nesting limits the phase space for low-energy particle-hole excitations, so that the SDW/CDW channel eventually saturates. In contrary, there is no phase-space restriction for Cooper pairing, and upon an attractive pairing interaction, either already existing or induced via the overlap to CDW/SDW channels, the SC channel is boosted via the Cooper mechanism until it diverges. Not surprisingly, we find s-SC/d-SC in relation to the subleading CDW/SDW channel. More interestingly, the negative isotope effect for CDW and SDW clearly also acts on the proximiting SC, as is clear in Figs. 7(c) and 7(d), and this is understood as from the channel overlap. The exception is the case of $\omega_D = 0.1$ in Fig. 7(c), which has the lowest T_c. In fact this is a case in the BCS limit, since $\lambda \ll 1$ and $\omega_D \ll W$.

[1] J. Bardeen, L. N. Cooper, and J. R. Schrieffer, Phys. Rev. **108**, 1175 (1957).

[2] R. Shankar, Rev. Mod. Phys. **66**, 129 (1994).

[3] A. B. Migdal, Sov. Phys. JETP **7**, 996 (1958); G. M. Eliashberg, *ibid.* **11**, 696 (1960).

[4] D. J. Scalapino, J. R. Schrieffer, and J. W. Wilkins, Phys. Rev. **148**, 263 (1966); W. L. McMillan, *ibid.* **167**, 331 (1968).

[5] A. J. Heeger, S. Kivelson, J. R. Schrieffer, and W. P. Su, Rev. Mod. Phys. **60**, 781 (1988).

[6] B. Batlogg, R. J. Cava, A. Jayaraman, R. B. van Dover, G. A. Kourouklis, S. Sunshine, D. W. Murphy, L. W. Rupp, H. S. Chen, A. White, K. T. Short, A. M. Mujsce, and E. A. Rietman, Phys. Rev. Lett. **58**, 2333 (1987); J. P. Franck, S. Harker, and J. H. Brewer, *ibid.* **71**, 283 (1993); D. Zech, H. Keller, K. Conder, E. Kaldis, E. Liarokapis, N. Poulakis, and K. A. Mller, Nature (London) **371**, 681 (1994).

[7] G.-m. Zhao, M. B. Hunt, H. Keller, and K. A. Muller, Nature (London) **385**, 236 (1997); H. Keller, Physica B (Amsterdam) **326**, 283 (2003); G.-H. Gweon, T. Sasagawa, S. Y. Zhou, J. Graf, H. Takagi, D.-H. Lee, and A. Lanzara, Nature (London) **430**, 187 (2004); J. Lee, K. Fujita, K. McElroy, J. A. Slezak, M. Wang, Y. Aiura, H. Bando, M. Ishikado, T. Masui, J.-X. Zhu, A. V. Balatsky, H. Eisaki, S. Uchida, and J. C. Davis, *ibid.* **442**, 546 (2006).

[8] A. S. Alexandrov, *Theory of Superconductivity: From Weak to Strong Coupling* (CRC Press, Boca Raton, 2003); K. A. Müller, J. Supercond. Nov. Magn. **27**, 2163 (2014).

[9] R. H. Liu, T. Wu, G. Wu, H. Chen, X. F. Wang, Y. L. Xie, J. J. Ying, Y. J. Yan, Q. J. Li, B. C. Shi, W. S. Chu, Z. Y. Wu, and X. H. Chen, Nature (London) **459**, 64 (2009); P. M. Shirage, K. Kihou, K. Miyazawa, C.-H. Lee, H. Kito, H. Eisaki, T. Yanagisawa, Y. Tanaka, and A. Iyo, Phys. Rev. Lett. **103**, 257003 (2009).

[10] Y. Takada and A. Chatterjee, Phys. Rev. B **67**, 081102 (2003); R. T. Clay and R. P. Hardikar, Phys. Rev. Lett. **95**, 096401 (2005); R. P. Hardikar and R. T. Clay, Phys. Rev. B **75**, 245103 (2007); M. Hohenadler and F. F. Assaad, *ibid.* **87**, 075149 (2013).

[11] G. Sangiovanni, M. Capone, C. Castellani, and M. Grilli, Phys. Rev. Lett. **94**, 026401 (2005); P. Paci, M. Capone, E. Cappelluti, S. Ciuchi, C. Grimaldi, and L. Pietronero, *ibid.* **94**, 036406 (2005); P. Paci, M. Capone, E. Cappelluti, S. Ciuchi, and C. Grimaldi, Phys. Rev. B **74**, 205108 (2006); G. Sangiovanni, O. Gunnarsson, E. Koch, C. Castellani, and M. Capone, Phys. Rev. Lett. **97**, 046404 (2006); P. Werner and A. J. Millis, *ibid.* **99**, 146404 (2007).

[12] J. Bauer and A. C. Hewson, Phys. Rev. B **81**, 235113 (2010); Y. Murakami, P. Werner, N. Tsuji, and H. Aoki, *ibid.* **88**, 125126 (2013).

[13] W.-S. Wang, Y.-Y. Xiang, Q.-H. Wang, F. Wang, F. Yang, and D.-H. Lee, Phys. Rev. B **85**, 035414 (2012).

[14] Y.-Y. Xiang, W.-S. Wang, Q.-H. Wang, and D.-H. Lee, Phys. Rev. B **86**, 024523 (2012).

[15] J. Friedel, J. Phys. Condens. Matter **1**, 7757 (1989).

[16] S. Barisić and O. Barisić, J. Superconduc. Novel Magnetism **25**, 669 (2012).

[17] W. Metzner, M. Salmhofer, C. Honerkamp, V. Meden, and K. Schznhammer, Rev. Mod. Phys. **84**, 299 (2012).

[18] C. Platt, W. Hanke, and R. Thomale, Adv. Phys. **62**, 453 (2013).

[19] C. N. Yang and S. C. Zhang, Mod. Phys. Lett. B **04**, 759 (1990).

[20] G. Mahan, *Many-Particle Physics* (Plenum Press, New York, 1981).

[21] E. A. Nowadnick, S. Johnston, B. Moritz, R. T. Scalettar, and T. P. Devereaux, Phys. Rev. Lett. **109**, 246404 (2012).
[22] D. J. Scalapino, E. Loh Jr, and J. E. Hirsch, Phys. Rev. B **34**, 8190 (1986).
[23] N. E. Bickers, D. J. Scalapino, and S. R. White, Phys. Rev. Lett. **62**, 961 (1989).
[24] C. Honerkamp, H. C. Fu, and D.-H. Lee, Phys. Rev. B **75**, 014503 (2007).
[25] R. M. Noack, D. J. Scalapino, and R. T. Scalettar, Phys. Rev. Lett. **66**, 778 (1991).
[26] A. Macridin, B. Moritz, M. Jarrell, and T. Maier, Phys. Rev. Lett. **97**, 056402 (2006).
[27] C.-H. Pao and H.-B. Schüttler, Phys. Rev. B **57**, 5051 (1998).
[28] N. D. Mermin and H. Wagner, Phys. Rev. Lett. **17**, 1133 (1966).
[29] J. M. Kosterlitz and D. J. Thouless, J. Phys. C: Solid State Phys. **6**, 1181 (1973).
[30] J. Zhong and H.-B. Schüttler, Phys. Rev. Lett. **69**, 1600 (1992).
[31] T. Sakai, D. Poilblanc, and D. J. Scalapino, Phys. Rev. B **55**, 8445 (1997).
[32] Z. B. Huang, W. Hanke, E. Arrigoni, and D. J. Scalapino, Phys. Rev. B **68**, 220507 (2003).
[33] A. S. Mishchenko and N. Nagaosa, Phys. Rev. Lett. **93**, 036402 (2004).
[34] A. Macridin, G. A. Sawatzky, and M. Jarrell, Phys. Rev. B **69**, 245111 (2004).
[35] C.-P. Chou and T.-K. Lee, Phys. Rev. B **81**, 060503 (2010); **85**, 104511 (2012).
[36] Z. B. Huang, H. Q. Lin, and E. Arrigoni, Phys. Rev. B **83**, 064521 (2011).
[37] A. Macridin, B. Moritz, M. Jarrell, and T. Maier, J. Phys. Condens. Matter **24**, 475603 (2012).
[38] A. Macridin and M. Jarrell, Phys. Rev. B **79**, 104517 (2009).
[39] C. Honerkamp, M. Salmhofer, N. Furukawa, and T. Rice, Phys. Rev. B **63**, 035109 (2001).
[40] W.-S. Wang, Y. Yang, and Q.-H. Wang, Phys. Rev. B **90**, 094514 (2014).